

PAPER • OPEN ACCESS

Seismic Assessment and Retrofit Design of a School Building in Florence

To cite this article: Gloria Terenzi *et al* 2019 *IOP Conf. Ser.: Mater. Sci. Eng.* **603** 032003

View the [article online](#) for updates and enhancements.

Seismic Assessment and Retrofit Design of a School Building in Florence

Gloria Terenzi ¹, Caterina Bazzani ¹, Iacopo Costoli ², Stefano Sorace ², Paolo Spinelli ¹

¹ Department of Civil and Environmental Engineering, University of Florence, 50139 Florence, Italy

² Polytechnic Department of Engineering and Architecture, University of Udine, 33100 Udine, Italy

iacopocostoli@gmail.com

Abstract. The recent earthquakes occurred in Italy highlighted again the high vulnerability of structures built before the release of national Seismic Standards. This induced several local authorities to undertake extensive performance assessment campaigns of public buildings, among which mainly schools. A study carried out within one of these campaigns, concerning the evaluation of seismic vulnerability and the design of retrofit interventions in a school building in Florence, is presented herein. The structure was built at the beginning of 1970s, and is characterized by a ground storey with reinforced concrete frame skeleton, and a first and second storey with steel structure. An extensive on-site experimental investigation was developed at a first step of the study, which allowed identifying the mechanical characteristics of the constituting materials, and re-drawing the main structural details. Based on these data, a check of the seismic performance in current conditions was carried out, which highlighted several drawbacks, especially concerning the steel members. This prompted to propose a seismic retrofit hypothesis of the building, consisting in the installation of a set of dissipative braces incorporating fluid viscous dampers as protective devices. A synthesis of the assessment analyses in current conditions and the retrofit design, which allows attaining an elastic structural response up to the maximum considered earthquake level, is reported in the paper.

1. Introduction

The high vulnerability of the Italian building stock designed before the release of national Seismic Standards, highlighted again by the earthquakes that hit Marche, Umbria and Lazio regions beginning from August 2016, induced local authorities to promote seismic performance assessment campaigns for public buildings, including schools.

The study presented in this paper, concerning a school built in Florence in the early 1970s, belongs to this line of activity. The structure is geometrically regular in elevation, and is constituted by a reinforced concrete (R/C) frame skeleton on the ground storey, and reticular steel beams and columns on the first and second storey. A detailed seismic assessment analysis carried out in current conditions showed some deficiencies in bending-compression stress states of several R/C and steel columns, as well as a buckling-affected response of the steel profiles, at the basic design earthquake (BDE) level.

This relatively poor performance prompted to propose a retrofit solution of the building, consisting in the installation of a dissipative bracing system incorporating silicone fluid-viscous (FV) devices.



The design objective of the intervention is represented by the attainment of an elastic response of the structure up to the maximum considered earthquake (MCE) normative level.

Details of the geometrical and structural characteristics of the case study building, as derived from a careful preliminary investigation campaign carried out on it, as well as of the performance assessment analyses and the retrofit design hypothesis, are offered in the next Sections.

2. Case study school building

Figure 1 shows the school building plan, with maximum external dimensions of (43.9×16.3) m×m. The average floor area is about 700 m², and the total volume is 8300 m³. As highlighted by the cross sections in figures 2 and 3, the storey heights are equal to 3.3 m (ground storey) and 3.75 m (upper storeys).

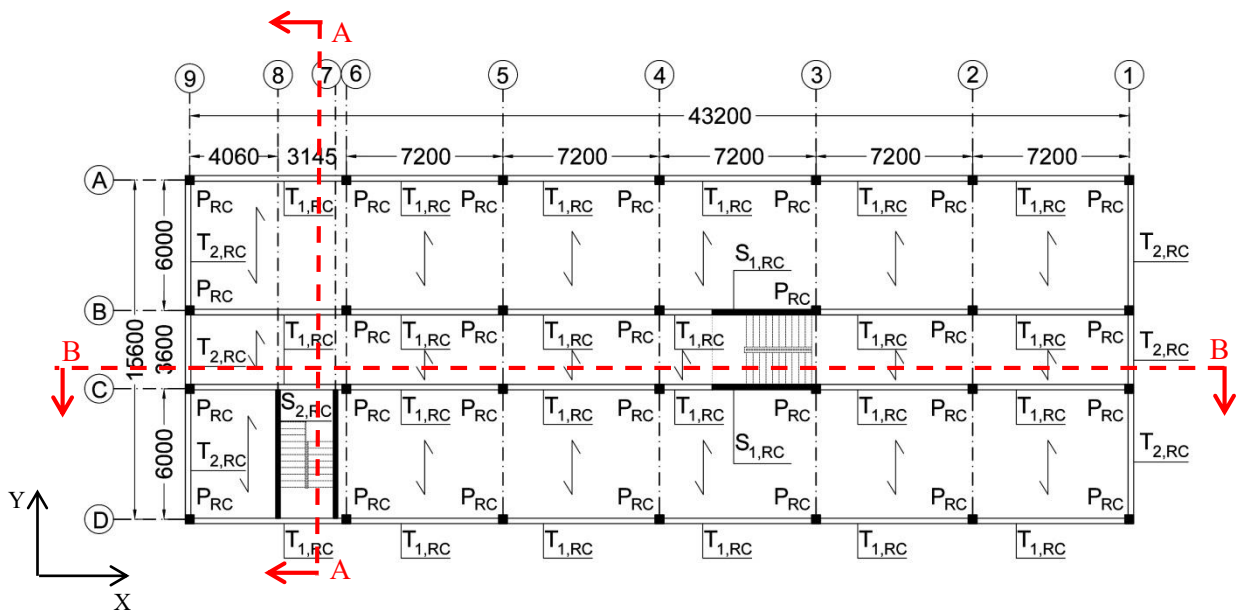


Figure 1. Ground floor plan with alphanumerical alignment identification and R/C beam numbering

An extensive on-site testing campaign was carried out on the building to identify the mechanical characteristics of the constituting materials and re-draw the main structural details, starting from the original design documentation. The on-site testing programme consisted in: core drillings in the basement, cover meter and rebar detection surveys, and extraction of reinforcement samples in the ground storey, for the R/C members; microdurometer and magnetic particle inspection tests on the welds, for the steel elements.

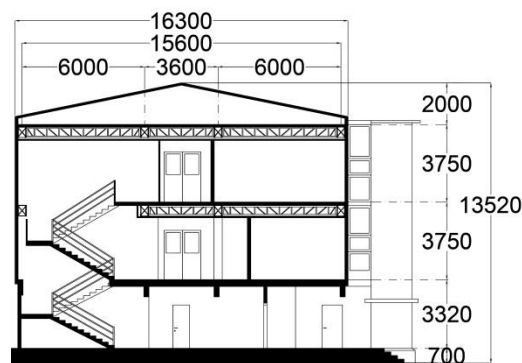


Figure 2. Transversal section of the building (denoted as A-A in Figure 1)

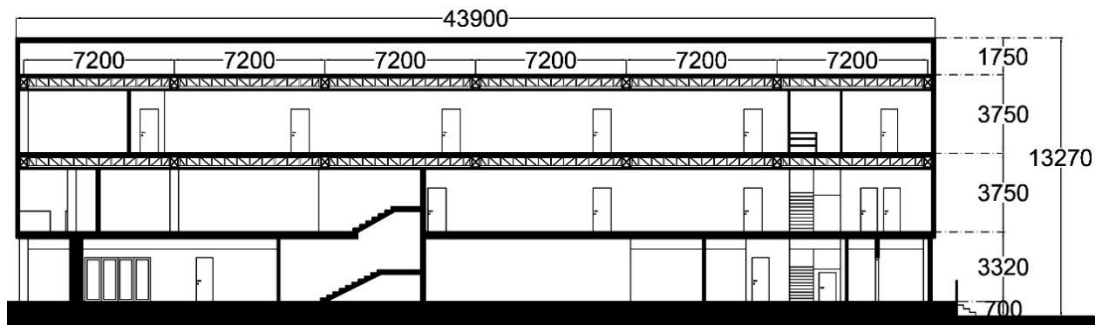


Figure 3. Longitudinal section of the building (denoted as B-B in Figure 1)

According to the nomenclature in Figure 1, and as illustrated in figure 4, beams $T_{1,RC}$ have cross section of (250×740) mm×mm and are reinforced by $\phi 12$ circular bars and square bars with side of 10 mm, and 8 mm square stirrups; beams $T_{2,RC}$ have section of (250×740) mm×mm, with 18 mm square bars and 8.5 mm square stirrups. R/C columns have section of (400×400) mm×mm, with 18 mm square bars and $\phi 8$ circular stirrups. $S_{I,RC}$ walls have section of (5900×200) mm×mm, with $\phi 12$ bars and $\phi 8$ transversal bars. The floors are of R/C “Predalles” type on the ground floor, and constituted by prefabricated R/C joists on the upper floors.

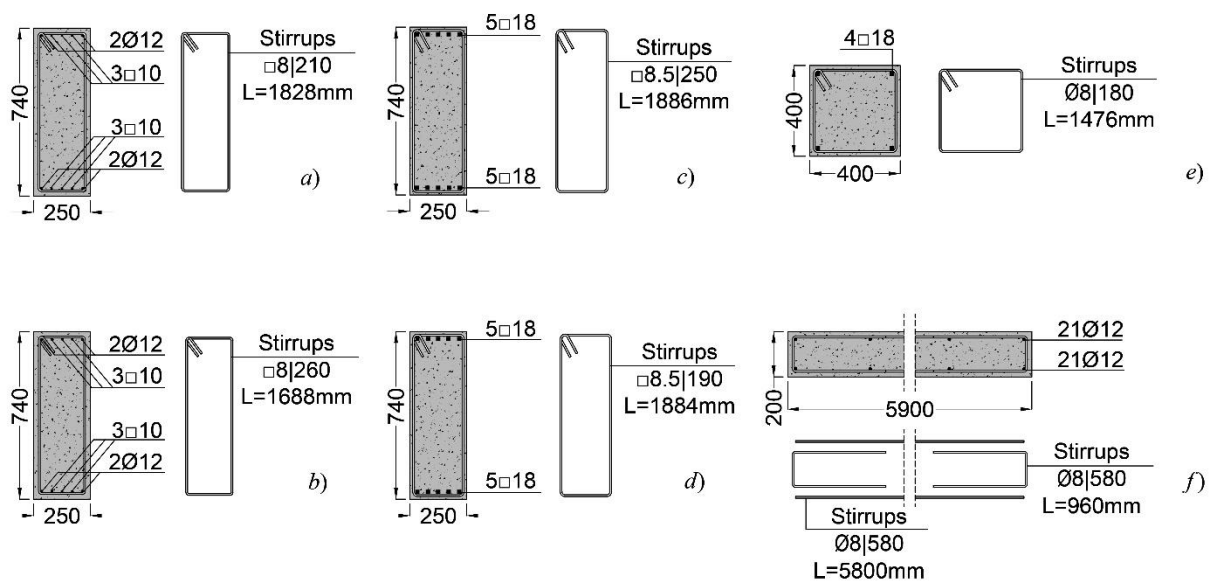


Figure 4. $T_{1,RC}$, (a-b) and $T_{2,RC}$ (c-d) beam sections at half-span (a-c) and at the ends (b-d); P_{RC} column section (e); $S_{I,RC}$ wall section (f)

As shown in the plans of figures 5 and 6, the reticular steel members of the first and second storey include seven different types of beams, displayed in figure 7, and a single type of column, detailed in figure 8. Based on the prescriptions of the Italian Technical Standards [1-2], the output of the testing campaigns allowed meeting the highest “knowledge level” for the structural system, named LC3. The corresponding “confidence factor” FC, i.e. the additional knowledge level-related safety coefficient to be introduced in the stress state checks, is equal to 1. The following mechanical properties of the constituting materials resulted from the characterization tests: mean cubic compressive strength of concrete equal to 21.5 N/mm²; yield stress of reinforcing steel bars equal to 421 MPa; yield stress of the steel members equal to 235 MPa.

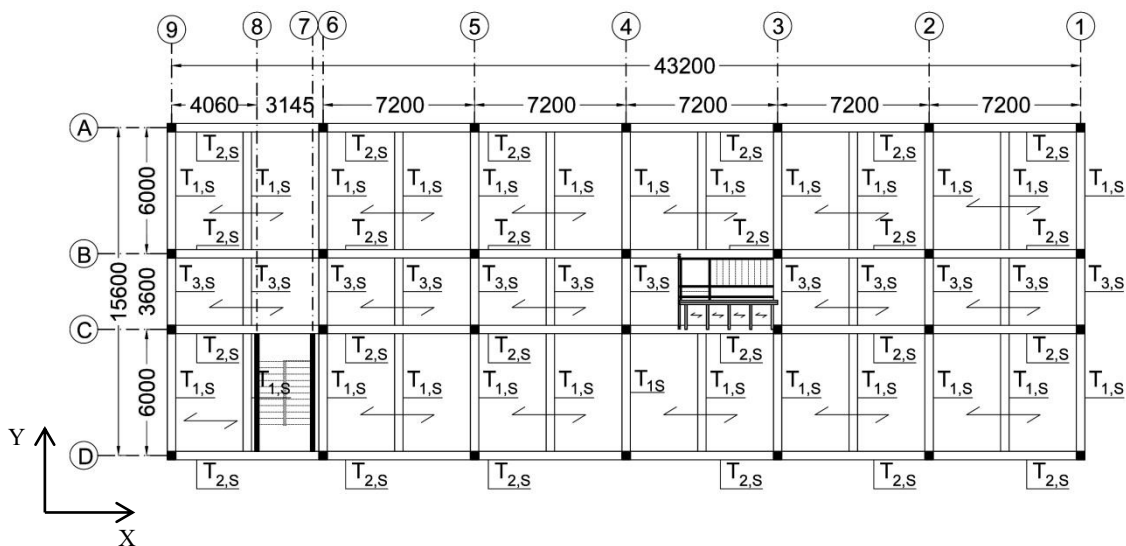


Figure 5. First floor plan with alphanumeric alignment identification and steel beam numbering

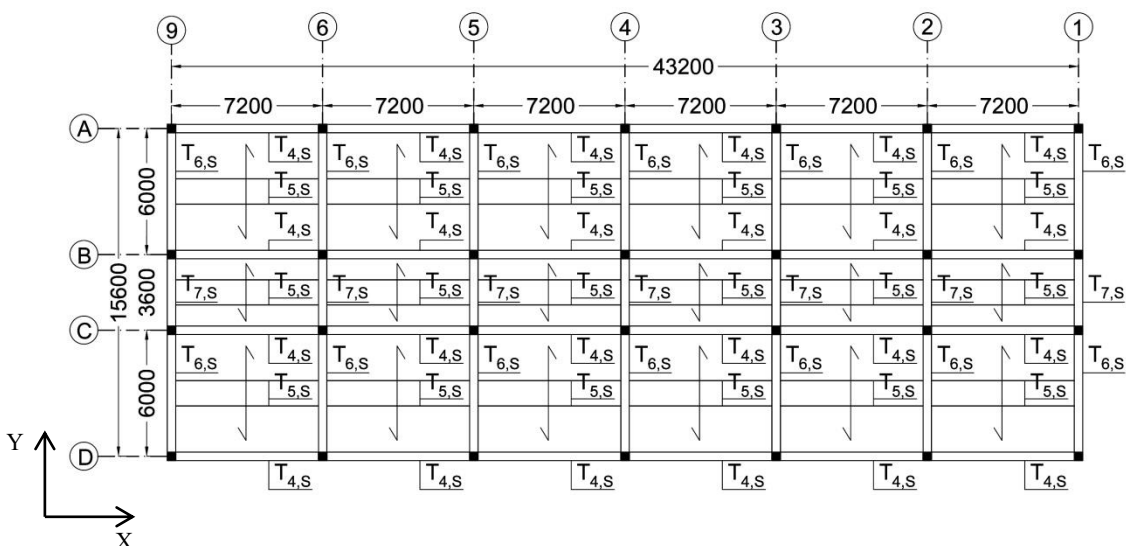


Figure 6. Roof plan with alphanumeric alignment identification and steel beam numbering

3. Assessment analysis in current conditions

The verification enquiry in current conditions is articulated in a modal analysis, to calculate the vibration periods and associated modal masses, and a time-history analysis, to assess the seismic performance of the structure in terms of stress states and displacements.

3.1 Modal analysis

The finite element models of the structure were generated by SAP2000NL calculus program [3], using frame type elements for all members. The cladding panels were considered as equivalent concentrated loads at the ends of the steel beams. At a first step, a complex model (CM – figure 9) was generated, by which the exact geometry of the steel beams and columns was reproduced. At a second step, a simplified model (SM – figure 10) was devised, with the aim of significantly reducing the computational effort of the analyses, where the reticular members were replaced by frame elements with inertial properties equivalent to the ones of beams and columns.

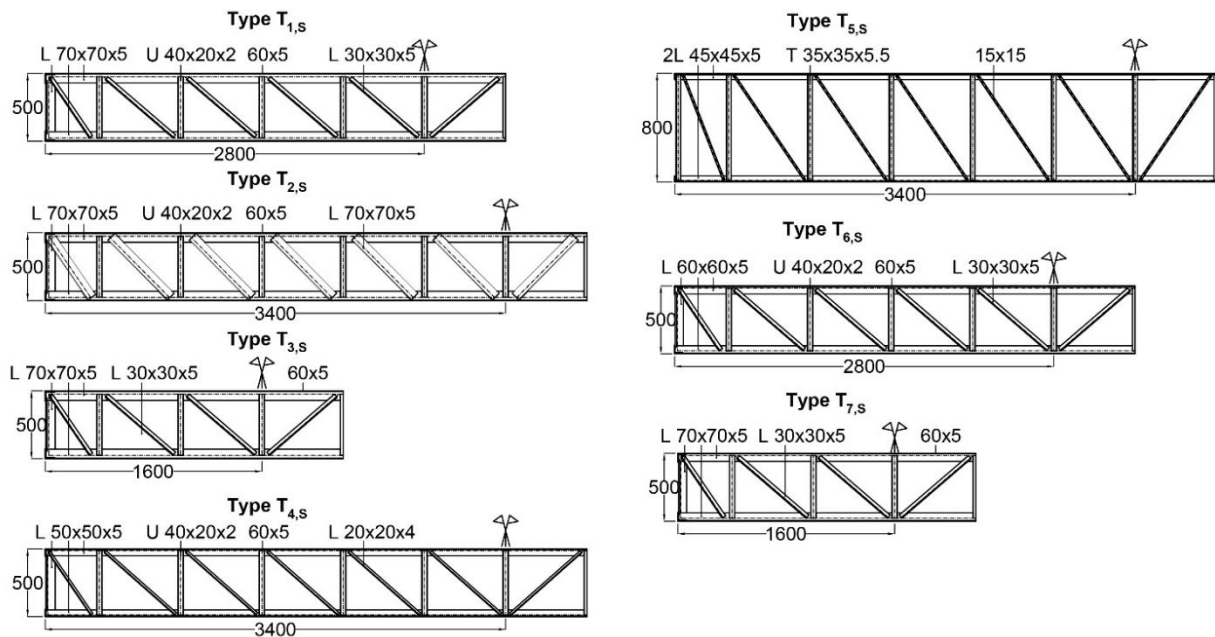


Figure 7. First and second storey reticular steel beams (types $T_{1,s}$, $T_{2,s}$, $T_{3,s}$, $T_{4,s}$, $T_{5,s}$, $T_{6,s}$, $T_{7,s}$)

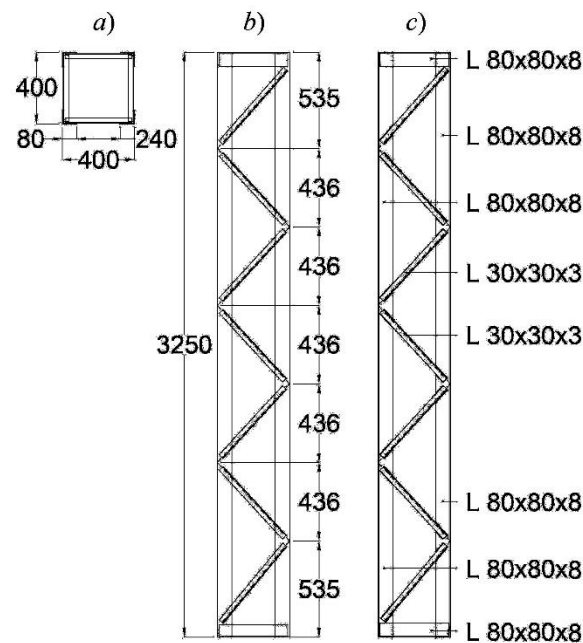


Figure 8. Steel columns; cross section (a), lateral view (b), and constituting profiles (c)

The effectiveness of the SM model was checked by comparing its first three modal periods with the corresponding periods obtained for the CM model. Relevant values are as follows: $T_1^{SM} = 0.61$ s (mixed rotational mode around Z-translational mode along Y); $T_2^{SM} = 0.30$ s (translational mode along X); $T_3^{SM} = 0.24$ s (mixed rotational mode around Z-translational mode along Y), for the SM model; and $T_1^{CM} = 0.60$ s (mixed rotational mode around Z-translational mode along Y mode); $T_2^{CM} = 0.36$ s (translational mode along X); $T_3^{CM} = 0.26$ s (mixed rotational mode around Z-translational mode along Y), for the CM model. The correlation is acceptably satisfactory, with maximum differences of 16.6% on the second mode and 7.7% on the third mode (the first mode periods virtually coincide).

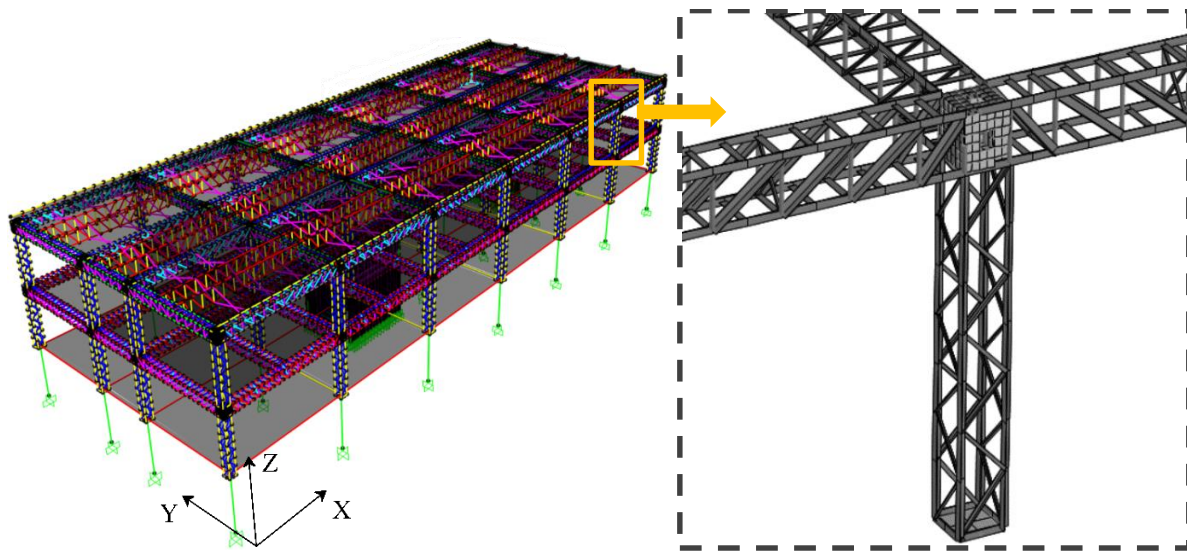


Figure 9. View of the CM finite element model of the structure and detail of a steel beam-to-column joint

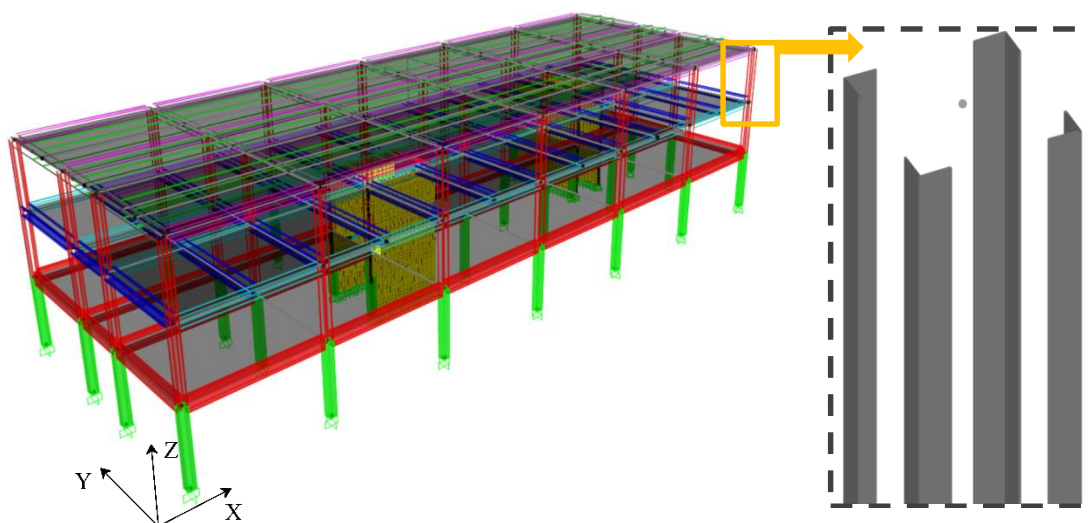


Figure 10. View of the SM finite element model of the structure and detail of an equivalent frame element adopted to schematize the reticular columns

The stress states (axial forces, shears and bending moments) obtained from the analyses carried out with the SM model are applied to the reticular columns as shown in figure 11, so as to check the stress conditions of the constituting profiles.

3.2 Time-history verification and performance assessment analysis

The performance evaluation analysis was carried out for the four reference seismic levels fixed in the Italian Standards [1], that is, Frequent Design Earthquake (FDE, with 81% probability of being exceeded over the reference time period V_R); Serviceability Design Earthquake (SDE, with 50%/ V_R probability); Basic Design Earthquake (BDE, with 10%/ V_R probability); and Maximum Considered Earthquake (MCE, with 5%/ V_R probability). The V_R period is fixed at 75 years, which is obtained by

multiplying the nominal structural life V_N of 50 years by a coefficient of use C_u equal to 1.5, imposed to school buildings.

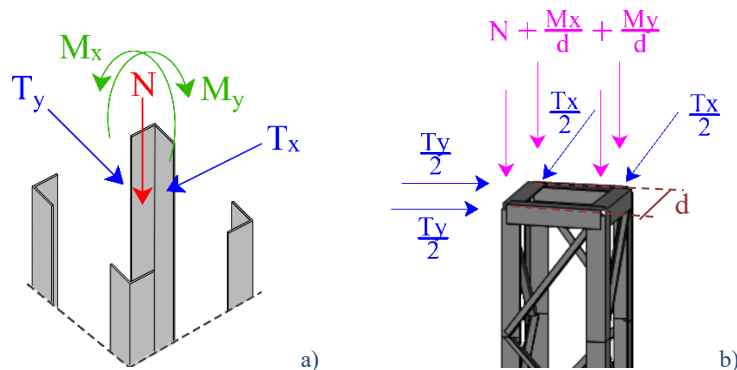


Figure 11. Stress patterns acting on the equivalent column section (a) and the reticular element (b)

By referring to topographic category T1 (flat surface), and B-type soil, the resulting peak ground accelerations for the four seismic levels referred to the city of Florence are as follows: 0.065 g (FDE), 0.078 g (SDE), 0.181 g (BDE), and 0.227 g (MCE). For the development of the time-history analyses, two families of seven accelerograms were generated from the pseudo-acceleration elastic spectral referred to Florence, plotted in figure 12. In each analysis, the accelerograms were applied in groups of two simultaneous horizontal components, with the first one selected from the first generated family of seven motions, and the second one selected from the second family.

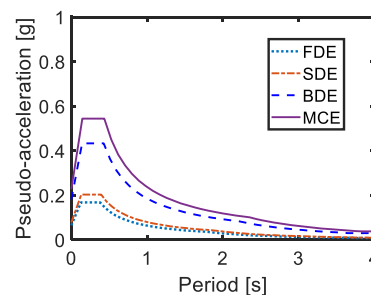


Figure 12. Normative pseudo-acceleration elastic response spectra for the site of Florence

The results of the analyses carried out at the SDE level were evaluated in terms of maximum inter-storey drift ratio (i.e. the ratio of the maximum inter-storey drift to the inter-storey height), ID_{max} , showing ID_{max} values below the Immediate Occupancy level-related threshold, ID_{IO} , equal to 0,5%. On the other hand, the axial force buckling limits computed for the vertical 80×8 mm×mm L-profiles and the diagonal 30×3 mm×mm L-profiles of columns, equal to 279.6 kN and 33.3 kN, respectively, are exceeded by factors equal to 2.75 – vertical profiles – and 2.2 – diagonal profiles –, at the BDE.

4. Retrofit hypothesis

Based on the results of the assessment analysis in current conditions, a retrofit solution was designed with the aim of significantly improving the seismic performance of the structure. The intervention hypothesis consists in the installation of a dissipative bracing system incorporating FV spring-dampers along both directions in plan, namely in the following vertical alignments (according to the nomenclature in figures 1, 5 and 6): A9-A6, A5-A4, A4-A3, A2-A1, D9-D6, D5-D4, D4-D3, D2-D1 in X , and 9A-9B, 9B-9C, 9C-9D, 1A-1B, 1B-1C, 1C-1D in Y , on the ground storey; A9-A6, A5-A4, A4-A3, A2-A1, D9-D6, D5-D4, D4-D3, D2-D1 in X , and 9A-9B, 9C-9D, 1A-1B, 1C-1D in Y , on the first and second storey. A view of the finite element model including the protection system is shown in figure 13.

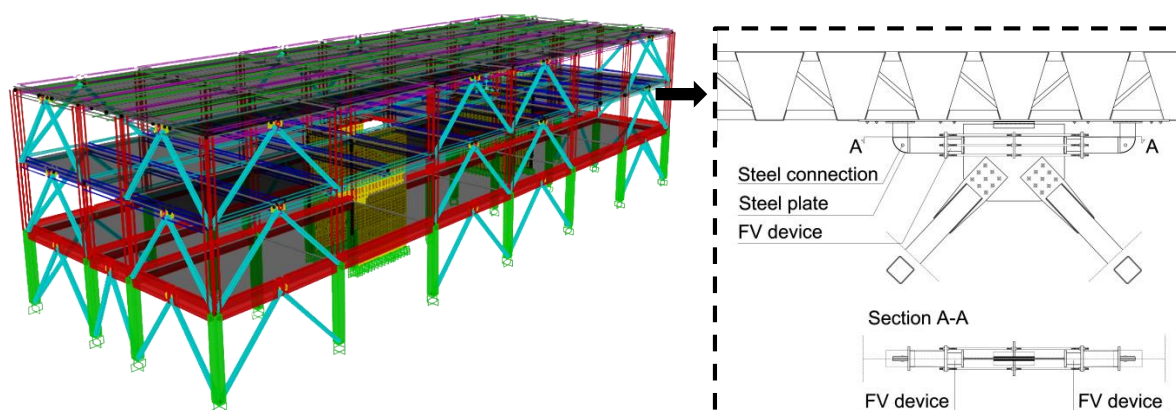


Figure 13. Finite element model of the structure incorporating the dissipative bracing system and installation details of the latter

4.1 Mechanical characteristics of the FV dampers

According to the general layout of the protective system, conceived for applications to several different types of structures and infrastructures [4-6], and illustrated by the drawing displayed in figure 13 for the considered building, the FV devices are installed in pairs at the tip of the supporting diagonal trusses, with inverted V-shaped layout. Differently from other classes of dissipaters, FV spring-dampers provide a very high damping action with small stiffening effects, which represents an effective property for rather stiff structures, like the case study one. The mechanical behaviour of FV devices is characterized by the following damping and elastic response force components [7]:

$$F_d = c \cdot \operatorname{sgn}[\dot{x}(t)] |\dot{x}(t)|^\alpha \quad (1)$$

$$F_{ne}(t) = k_2 x(t) + \frac{(k_1 - k_2) x(t)}{\left[1 + \left| \frac{k_1 x(t)}{F_0} \right|^5 \right]^{1/5}} \quad (2)$$

where: t = time variable; c = damping coefficient; $\operatorname{sgn}(\cdot)$ = signum function; $\dot{x}(t)$ = velocity; $|\cdot|$ absolute value; α = fractional exponent, ranging from 0.1 to 0.2; F_0 = static pre-load; k_1, k_2 = stiffness of the response branches situated below and beyond F_0 ; $x(t)$ = displacement.

4.2 Sizing design procedure of the FV dampers and performance verification in retrofitted conditions

The design procedure applied for preliminarily sizing the FV devices is based on the assumption that, as observed above, for relatively stiff frame structures a substantial improvement of seismic performance can be reached by incorporating a supplemental damping system with limited stiffening capacity. For more deformable structures, a supplemental stiffness contribution helps control lateral displacements better, and prevents over-dissipation demands to the protective technology adopted.

The FV spring-dampers were designed by following the sizing procedure proposed in [8], and referring to its implementation for structures with poor shear and/or bending moment strength of the constituting members. As discussed in this Section, the design methodology can be extended to reticular steel elements, like the ones forming the skeleton of the two upper storeys of the case study building, normally affected by low critical (i.e. Eulerian stability-related) axial force capacity of the member profiles. The procedure starts by assuming prefixed reduction factors, α_s , of the highest response parameters in current conditions, which are evaluated by means of a conventional elastic finite element analysis. Simple formulas relating the reduction factors to the equivalent viscous damping ratio of the dampers, ξ_{eq} , allow calculating the ξ_{eq} values that guarantee the achievement of the target reduction factors. Finally, the energy dissipation capacity of the devices is deduced from ξ_{eq} , finalizing their sizing process.

The peculiarity of the application of the design procedure to the examined structure is represented by the fact that in this case, as observed above, α_s must be computed by considering the possible axial instability of the profiles constituting the reticular steel columns. Therefore, said M_{tj}^a (or N_{tj}^a) the maximum moment (or axial force) evaluated in current conditions for the most stressed truss element of the columns in the j -th storey, and M^R (or N^{cr}) the corresponding limit resistance moment (or critical axial force) value, the α_s ratio is given by:

$$\alpha_s = \frac{M_{tj}^a}{M^R} \quad \text{or} \quad \alpha_s = \frac{N_{tj}^a}{N^{cr}} \quad (3)$$

By introducing this relation in the ξ_{eq} equation [8]:

$$\xi_{eq} = \frac{2(\alpha_s - 1)}{\pi \alpha_s} \quad (4)$$

and substituting ξ_{eq} in the dissipated energy expression

$$E_D = 2\pi\alpha_s F_e \xi_{eq} d_{d,max} \quad (5)$$

where: F_e = elastic base shear of the structure, and $d_{d,max}$ = maximum displacement of the devices, the energy dissipation to be assigned to the FV dampers is estimated by (5). Then, the devices with the nearest energy dissipation capacity, as identified from the manufacturer's catalogue [10], are tentatively selected.

Alternatively, the energy dissipation demand on the FV dampers can be calculated by referring to the ratio of the maximum inter-storey drift to the relevant drift limitation imposed by the Technical Standards for the considered performance level; the corresponding response reduction ratio, α_d , the ξ_{eq} equation and the dissipated energy expression are given by:

$$\alpha_d = \frac{ID_{max}}{ID_e} \quad (6)$$

$$\xi_{eq} = \frac{2(\alpha_d - 1)}{\pi} \quad (7)$$

$$E_D = 2\pi F_e \xi_{eq} ID_e \quad (8)$$

The verification analysis in current conditions highlights that the most stressed columns of all storeys are 1B, for bending moments around Y , and 1C, for bending moments around X , respectively. In the theoretical hypothesis of indefinitely elastic behaviour of the material, for the MCE-scaled seismic action applied to the SM model the M_{tj}^a value on the ground storey, M_{tGS}^a , would be equal to 68 kNm in column 1B around Y ($M_{tGS,Y}^a$), and 290.9 kNm in column 1C around X ($M_{tGS,X}^a$). The corresponding ultimate values are as follows: $M_{SG,Y}^R = 26.88$ kNm (computed for the concurrent axial force $N^R = 390.2$ kN); and $M_{SG,X}^R = 128.2$ kNm ($N^R = 403.6$ kN). The maximum bending moment around X for the most stressed column on the first storey, $M_{tIS,X}^a$, is equal to 149.4 kNm, i.e. remarkably greater than the corresponding ultimate value, equal to 96.1 kNm. Critical axial force conditions are checked on the first storey along X , in a diagonal truss of column 1C, for which the computed axial force $N_{tIS,X}^a$ is equal to 73.9 kN, as compared to a corresponding critical axial force, N_{diag}^{cr} , of 33.3 kN. Concerning the second storey, the most demanding conditions are determined by the axial force in the vertical profiles of column 1C, in X direction ($N_{tIS,X}^a = 450.6$ kN vs $N_{vert}^{cr} = 279.6$ kN), and by the drifts, in Y . For the latter, maximum values of 43 mm are noticed, as compared to an elastic drift limit of 19 mm.

Based on the results for the three storeys, the following reduction factors α_s and α_d are computed: $\alpha_{s,GSM,X} = 2.53$, $\alpha_{s,GSM,Y} = 2.26$ (ground storey); $\alpha_{s,ISN,X} = 2.22$, $\alpha_{s,ISM,Y} = 1.55$ (first storey); and $\alpha_{s,IISN,X} = 1.60$, $\alpha_{s,IISd,Y} = 2.26$ (second storey). The corresponding equivalent viscous damping ratios of the sets of FV spring-dampers to be installed on the three levels, calculated by means of relations (4) and (7), are: $\xi_{eq,SG,X} = 0.38$, $\xi_{eq,SG,Y} = 0.35$, $\xi_{eq,IS,X} = 0.35$, $\xi_{eq,IS,Y} = 0.23$, $\xi_{eq,IIS,X} = 0.24$, and $\xi_{eq,IIS,Y} = 0.80$. The E_D energy

dissipation capacities of the spring–dampers are consequently computed by relations (5) and (8), for the following values of the elastic limit shear of the j -th storey (given by the sum of the elastic limit shear forces of all columns belonging to the same storey) in X , $F_{ej,X}$, and Y , $F_{ej,Y}$: $F_{eGS,Y}=3502.3$ kN; $F_{eGS,X}=4097.8$ kN, $F_{eIS,X}=F_{eIS,Y}=F_{eIIS,X}=F_{eIIS,Y}=4288.2$ kN, and the corresponding drifts limits: $ID_{e,SG}=d_{dGS,max}=16$ mm; $ID_{e,SI}=ID_{e,SII}=d_{dIS,max}=19$ mm. Therefore, the following tentative E_D values are estimated: $E_{D,SG,X}=395$ kJ, $E_{D,SG,Y}=278$ kJ, $E_{DIS,X}=397$ kJ, $E_{DIS,Y}=182$ kJ, $E_{DIIS,X}=409$ kJ, and $E_{DIIS,Y}=196$ kJ.

The design of the spring-dampers was finalized by referring to the total dissipated energy in the two directions: $E_{Dtot,X}=1201$ kJ, $E_{Dtot,Y}=656$ kJ. By dividing these values by the number of devices placed in X and Y , the maximum energy dissipation capacity $E_{D,X,dmax}$, $E_{D,Y,dmax}$, that should be assigned to each damper to reach the target performance at the MCE results as follows: $E_{D,X,max}=24.8$ kJ, $E_{D,Y,max}=23$ kJ. Assuming these energy values as sizing limits, the spring-damper type with the nearest nominal energy dissipation capacity E_n to $E_{D,j,max}$ has the following mechanical properties, as drawn from the manufacturer's catalogue [10]: $E_n=24$ kJ; stroke $s_{max}=\pm 50$ mm; damping coefficient $c=38$ kN/(s/mm) $^\gamma$, with $\gamma=0.15$; $F_0=60$ kN; and $k_2=1.55$ kN/mm.

Based on this assumption, a final seismic performance analysis in retrofitted conditions was carried out, which highlighted the attainment of the planned performance improvement. Indeed, the maximum drifts are reduced below the ID_e limits also in Y direction for the second storey, and moments and axial forces decrease up to the following values (in brackets are recapitulated the corresponding ultimate values): $M_{tGS,Y}^{RC}=50.0$ kNm ($M_{SG,Y}^R=57.8$ kNm); $M_{tGS,X}^{RC}=91.9$ kNm ($M_{SG,X}^R=115.8$ kNm); $M_{tIS,X}^{RC}=68.8$ kNm ($M_{IS,X}^R=96.1$ kNm); $N_{tIS,X}^{RC}=12.2$ kN ($N_{diag}^{cr}=33.3$ kN) in the diagonal profiles of column 1C on the first storey, and $N_{tIIS,X}^{RC}=268.3$ kN ($N_{vert}^{cr}=279.6$ kN) in the vertical profiles of column 1C on the second storey. These final results assess the effectiveness of the proposed design solution, which could be extended, in perspective, to other pre-normative buildings with similar characteristics.

Acknowledgments

The study reported in this paper was sponsored by the Italian Department of Civil Protection within the ReLUIS-DPC Project 2019/2021 – Work Package 15: Normative Contributions for Isolation and Dissipation. The authors gratefully acknowledge this financial support.

References

- [1] Italian Council of Public Works, “Technical Standards on Constructions,” *Italian Council of Public Works*: Rome, Italy, 2018.
- [2] Italian Council of Public Works, “Commentary on the Technical Standards on Constructions,” *Italian Council of Public Works*: Rome, Italy, 2019.
- [3] SAP2000NL, “Theoretical and Users’ Manual, Release 19.05,” *Computers & Structures Inc.*: Berkeley, CA, USA, 2018.
- [4] S. Sorace, and G. Terenzi, “Seismic protection of frame structures by fluid viscous damped braces,” *Journal of Structural Engineering ASCE*, vol. 134, n. 1, pp. 45-55, 2008.
- [5] S. Sorace, G. Terenzi, and C. Mori, “Passive energy dissipation-based retrofit strategies for R/C frame water storage tanks,” *Engineering Structures*, vol. 106, pp. 385-398, 2016.
- [6] S. Sorace, and G. Terenzi, “Existing prefab R/C industrial buildings: Seismic assessment and supplemental damping-based retrofit,” *Soil Dynamics and Earthquake Engineering*, vol. 94, pp. 193-203, 2017.
- [7] S. Sorace, and G. Terenzi, “Non-linear dynamic modelling and design procedure of FV spring-dampers for base isolation,” *Engineering Structures*, 23, 1556–1567, 2001.
- [8] G. Terenzi, “Energy-based design criterion of dissipative bracing systems for seismic retrofit of framed structures,” *Applied Sciences*, 2018, vol. 8, n. 268, doi:10.3390/app8020268.
- [9] G. Terenzi, “Dynamics of SDOF systems with nonlinear viscous damping,” *Journal of Engineering Mechanics ASCE*, vol. 125, n. 8, pp. 956-963, 1999.
- [10] Jarret, S.L., 2018. Shock-Control Technologies. Available online: <http://www.introini.info>.